**Structural Engineering and Mechanics**, *Vol. 50, No. 1 (2014) 73-88*
DOI: http://dx.doi.org/10.12989/sem.2014.50.1.073 

# Use of vibration characteristics to predict the axial deformation of columns

H.N. Praveen Moragaspitiya, David P. Thambiratnam*, Nimal J. Perera and Tommy H.T. Chan

*School of Civil Engineering & Built Environment, Queensland University of Technology, Brisbane, Australia*

*(Received June 19, 2013, Revised January 29, 2014, Accepted February 13, 2014)*

**Abstract.** Vibration characteristics of columns are influenced by their axial loads. Numerous methods have been developed to quantify axial load and deformation in individual columns based on their natural frequencies. However, these methods cannot be applied to columns in a structural framing system as the natural frequency is a global parameter of the entire framing system. This paper presents an innovative method to quantify axial deformations of columns in a structural framing system using its vibration characteristics, incorporating the influence of load tributary areas, boundary conditions and load migration among the columns.

**Keywords:** modal flexibility; axial deformation; load migration; dynamic stiffness matrix; load tributary areas

## 1. Introduction

Axially loaded structural components can be found in aerospace, civil and mechanical structural framing systems. Performance of such components and hence the structural framing system can be evaluated using vibration characteristics since the axial loads influence the vibration characteristics of the structural framing system. Several researchers (Yesilce and Demirdag 2008, Shaker 1975, Della and Shu 1975) have investigated the influence of axial loads on vibration characteristics of individual structural components with different boundary conditions and established a relationship between the frequency and the axial load. Their methods can be used to quantify axial force and or buckling load of a structural component using natural frequencies. However, as the natural frequency is a property of the entire structural framing system, these methods are limited to individual structural components. This is the main threshold in previous developments.

The influence of axial force on the vibration characteristics of modal vectors and natural frequencies of individual structural components has been treated in past researches. Yesilce and Demindag (2008) derived the first five natural frequencies and corresponding mode shapes of an axially loaded multi-span Timoshenko beam and showed that the frequencies decrease with the axial compressive force. This finding confirmed that the stiffness of the beam is influenced by the

*Corresponding author, Professor, E-mail: d.thambiratnam@qut.edu.au


http://www.techno-press.org/?journal=sem&subpage=8 ISSN: 1225-4568 (Print), 1598-6217 (Online)

axial force. NASA (National Aeronautics and Space Administration) technical note, NASA TN-D-8109 presented a numerical study on the effects of axial loads on the modal parameters of beams with different boundary conditions and showed that the natural frequencies reduce and the mode shapes change with increase in axial force (Shaker 1975). This study also indicated that the boundary conditions impact on mode shapes of the beam. Della and Shu (1975) showed that a monotonic relation exists between the natural frequency and the axial compressive force in beams. They also showed that the axial compressive force influences the mode shapes and that this influence reduces with the mode number. Walter and Kang (1996) investigated impact of axial force on vibration characteristics of a beam and developed a stiffness equation incorporating influence of axial force. Bahra *et al.* (2008) carried out a comprehensive study to examine axial load pattern updating using ambient vibration data from a physical frame. Equations developed by these authors were validated using ambient vibration data and confirmed that axial compressive force reduces the stiffness of the elements. Murat (2012) investigated the influence of axial forces on the behavior of the beams with cracks. Outcomes of his research confirmed that there is a significant impact of axial load on the dynamic characteristics. Moragaspitiya *et al.* (2012) studied the vibration properties of tall buildings comprising the belt and outrigger systems. In this study the influence of axial force on vibration properties of structural components and hence the whole structural framing system was investigated.

It is hence evident that axial forces have an effect on the natural frequencies and mode shapes of a structure. To the best of the authors' knowledge, none of the existing methods can solve the inverse problem to determine axial force and hence axial deformation of structural components in a structural framing system using its vibration characteristics. Moragaspitiya *et al.* (2010) highlighted the importance of including load migration due to horizontal structural systems such as belt and outrigger systems on the axial deformation of vertical structural components. This paper proposes an innovative and rigorous procedure to solve the inverse problem to determine these axial effects incorporating load migration based on the Modal Flexibility (MF) phenomenon which uses both modal vectors and natural frequencies.

Based on the literature review above, it is evident that the stiffness matrix changes due to the applied axial load so that the mode shapes and natural frequencies also change. Since MF is inversely proportional to stiffness, it is obvious that there is a relationship between MF and axial loads and axial deformation of the structural component. This paper will pursue such a relationship.

### *1.1 Modal flexibility*

The Modal Flexibility (MF) of a structure is indicative of its dynamic characteristics and incorporates both the modal vectors and natural frequencies. MF phenomenon has been widely used in performance assessment and damage detection of structures since it is accurate and convenient to apply. Shih *et al.* (2009) used the MF phenomenon to detect damage in flexural structural components. MF is used to develop the methodology proposed in this paper.

#### *1.1.1 Modal flexibility of an element*

Modal Flexibility $F_x$ of an element x of a structural component can be obtained as (Shih *et al.* 2009), Catbas *et al.* (2006), Zhao *et al.* (2006) and Adewuyi *et al.* (2010).

$$F_x = \sum_{r=1}^{n} \frac{1}{\omega_r^2} \phi_{xr} \phi_{xr}^T \tag{1}$$

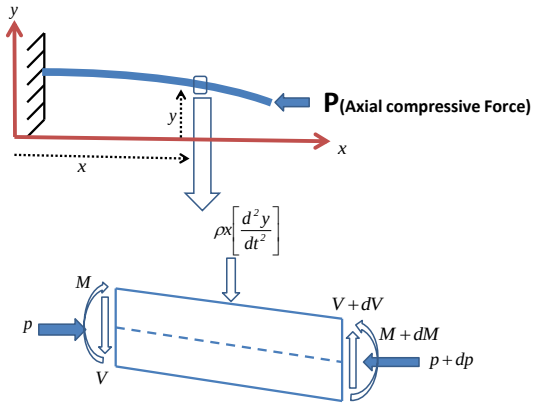


Fig. 1 Structural component with axial compressive force

Where

*r* and *n* = the mode and total number of modes respectively

$\Phi_{xr}$= modal vector of element *x* for mode *r*

Since, the $\omega^2$ term is in the denominator of Eq. (1), the modal contributions decrease with increasing frequencies, resulting in the rapid convergence of $F_x$.

## 2. Methodology

The following sets of Eqns. are derived to present the influence of axial force on modal vectors and natural frequencies of a structural component and hence extended to the entire structural framing system. A beam with fixed end and subjected to an axial compressive force as shown in Fig. 1 is considered,

where

*P*- axial compressive force

*M*-moment

*V*-Shear Force

ρ-mass per unit length

*y*,*x*-axial coordinates

*t*-time

For free vibration of this component, Eqs. (2) and (3) incorporating the axial force, moment and shear force can be derived.

$$\frac{dM}{dx} + P\left[\frac{dy(x,t)}{dx}\right] + V = 0 \tag{2}$$

$$\frac{dV}{dx} - \rho\left[\frac{d^2y(x,t)}{dt^2}\right] = 0 \tag{3}$$

From the beam theory

$$M = EI\left[\frac{d^2y(x,t)}{dx^2}\right] \tag{4}$$

Where EI- flexural rigidity of the component

Eqn. (5) can be derived using Eqs. (2), (3) and (4)

$$EI\left[\frac{d^4y(x,t)}{dx^4}\right] + P\left[\frac{d^2y(x,t)}{dx^2}\right] + \rho\left[\frac{d^2y(x,t)}{dt^2}\right] = 0 \tag{5}$$

Eq. (5) is a fourth order homogeneous differential equation. The solution $y(x,t)$ to this equation. can be expressed as in Eq. (6) where $Z(x)$ and $w(t)$ represent the influence of distance $x$ and time $t$ respectively

$$y(x,t) = Z(x)w(t) \tag{6}$$

Eq. (6) is substituted into Eq. (5) in order to form Eq. (7) as follows

$$\frac{EI\left[\frac{d^4Z(x)}{dx^4}\right] + P\left[\frac{d^2Z(x)}{dx^2}\right]}{[Z(x)]} = \frac{-\rho\left[\frac{d^2w(t)}{dt^2}\right]}{[w(t)]} = \omega^2 \tag{7}$$

where $\omega$- natural frequency

Solution of Eqn. (7) is

$$z(x) = D_1\sinh(\alpha_1 x) + D_2\cosh(\alpha_1 x) + D_3\sin(\alpha_2 x) + D_4\cos(\alpha_2 x) \tag{8}$$

Where

$$\alpha_1^2 = \frac{-P + \sqrt{p^2 + 4EI\omega^2}}{2EI} \tag{9}$$

$$\alpha_2^2 = \frac{-P - \sqrt{p^2 + 4EI\omega^2}}{2EI} \tag{10}$$

$D_1$, $D_2$, $D_3$, $D_4$- vector constants

and

$$w(t) = A_1\sin(\beta_1 t) + A_2\cos(\beta_2 t) \tag{11}$$

where

$$\beta_1 = \sqrt{\frac{\omega^2}{\rho}} \tag{12}$$

$$\beta_2 = -\sqrt{\frac{\omega^2}{\rho}} \tag{13}$$

$A_1$ ,$A_2$-constants determined from initial conditions of the vibration.

Displacement of the structural component under free vibration can be expressed as follows

$$y(x,t)=\{D_1 \sinh(\alpha_1 x)+D_2 \cosh(\alpha_1 x)+D_3 \sin(\alpha_2 x)+D_4 \cos(\alpha_2 x)\}w(t) \tag{14}$$

Considering boundary conditions and the initial conditions of vibration, Eqn. (15) can be formed as follows

$$\{Y\}=[A]\{D\} \tag{15}$$

Where

$$\{Y\}=\begin{Bmatrix} y(0,t) \\ y'(0,t) \\ y(L,t) \\ y'(L,t) \end{Bmatrix} \tag{16}$$

$$[A]=\begin{bmatrix} 0 & 1 & 0 & 1 \\ \alpha_1 & 0 & \alpha_2 & 0 \\ \sinh(\alpha_1 L) & \cosh(\alpha_1 L) & \sin(\alpha_2 L) & \cos(\alpha_2 L) \\ \alpha_1 \cosh(\alpha_1 L) & \alpha_1 \sinh(\alpha_1 L) & \alpha_2 \cos(\alpha_2 L) & -\alpha_2 \sin(\alpha_2 L) \end{bmatrix} \tag{17}$$

$$\{D\}=\begin{Bmatrix} \overline{D_1} \\ \overline{D_2} \\ \overline{D_3} \\ \overline{D_4} \end{Bmatrix} \tag{18}$$

Where $\overline{D_1}$, $\overline{D_2}$, $\overline{D_3}$, $\overline{D_4}$ -vector constants

Eqn. (19) can be written considering moment, *M* and shear force, *V*

$$\{F\}=[B]\{D\} \tag{19}$$

Where

$$\{F\}=\begin{Bmatrix} M_{x=0} \\ V_{x=0} \\ M_{x=L} \\ V_{x=L} \end{Bmatrix} \tag{20}$$

$$[B]=\begin{bmatrix} 0 & EI\alpha_1^2 & 0 & -EI\alpha_2^2 \\ -(p\alpha_1+EI\alpha_1^3) & 0 & -(p\alpha_2-EI\alpha_2^3) & 0 \\ EI\alpha_1^2 \sinh(\alpha_1 L) & EI\alpha_1^2 \cosh(\alpha_1 L) & -EI\alpha_2^2 EI \sin(\alpha_2 L) & -EI\alpha_2^2 EI \cos(\alpha_2 L) \\ -(p\alpha_1+EI\alpha_1^3)\cosh(\alpha_1 L) & -(p\alpha_1+EI\alpha_1^3)\sinh(\alpha_1 L) & -(p\alpha_2-EI\alpha_2^3)\cos(\alpha_2 L) & -(-p\alpha_2+EI\alpha_2^3)\sin(\alpha_2 L) \end{bmatrix} \tag{21}$$

$$M=EI\left[\frac{d^2 y(x,t)}{dx^2}\right] \tag{22}$$

and

$$V = -\left( \frac{dM}{dx} + P\left[ \frac{dy(x,t)}{dx} \right] \right) \tag{23}$$

Eq. (24) can be formed by using Eqs. (15) and (19) as follows

$$\{F\} = [B][A]^{-1}\{Y\} \tag{24}$$

$$\{F\} = [\bar{k}]_L\{Y\} \tag{25}$$

where $[\bar{k}]_L$ –dynamic stiffness matrix of the element and subscript, *L* indicates the local coordinate system.

The above stiffness matrix is defined based on the local coordinate system so that the transformation matrix, [*T*] can be employed (Friberg 1985) as follows to establish the stiffness matrix in the global coordinate system.

$$[\bar{k}]_G = [T]^T[\bar{k}]_L[T] \tag{26}$$

where subscript *G* refers to the global coordinate system

The dynamic stiffness matrix of the structure, $[\bar{K}]$, incorporating the influence of axial loads can then be formed by assembling stiffness matrices of the structural components considering compatibility of the nodes

With the use of the dynamic stiffness matrix $[\bar{K}]$, the Eqn. of free vibration of a structure with the influence of the axial forces in structural components can be represented as

$$[\bar{K}]\{\phi\} = \{0\} \tag{27}$$

where Φ- modal vector

It is clear from the above derivations that there is an impact of the axial compressive forces on the modal parameters of the components and the entire structural framing system. However, it is not convenient to solve Eq. (27) to examine the effects of modal parameters in a complex structural framing system with shear walls as shown in Example 3 (discussed in the next section).

The Finite Element (FE) Method is an accessible analysis tool in engineering areas as it can be used to capture the complex behaviour of structures. The preprocessing technique in the FE package, ANSYS (2011) is used along with the theory presented above to incorporate the axial effects of structural components into the modal analysis.

Modal Flexibility (MF) for an element (element *x*) without the axial load (unloaded case) can be written as (using Eq. (1))

$$F_{XU} = \left[ \sum_{r=1}^{n} \frac{1}{\omega_r^2} \phi_{xr} \phi_{xr}^T \right]_U \tag{28}$$

where subscript *U* denotes the unloaded case

The stiffness matrix of an element changes due to the influence of the axial force and consequently the modal parameters and MF of such an element also change. Modal Flexibility (MF) for element *x* with the axial load (loaded case) can be written as

$$F_{XL} = \left[ \sum_{r=1}^{n} \frac{1}{\omega_r^2} \phi_{xr} \phi_{xr}^T \right]_L \tag{29}$$

where subscript *L* denotes the loaded case

In order to amplify the effects of these modal flexibility changes, reciprocals of the two MFs for the unloaded and loaded cases are considered as shown below

$$\frac{1}{F_{XU}} = \frac{1}{\left[ \sum_{r=1}^{n} \frac{1}{\omega_r^2} \phi_{xr} \phi_{xr}^T \right]_U} \tag{30}$$

$$\frac{1}{F_{XL}} = \frac{1}{\left[ \sum_{r=1}^{n} \frac{1}{\omega_r^2} \phi_{xr} \phi_{xr}^T \right]_L} \tag{31}$$

To capture the influence of the axial force on the MF or the vibration characteristics, the parameter, *SI* called the stiffness index is introduced through Eq (32). This parameter is directly proportional to the stiffness reduction which occurs due to the axial load.

$$SI = \frac{1}{F_{XU}} - \frac{1}{F_{XL}} \tag{32}$$

This stiffness Index (*SI*) can be implemented for a structure using the procedure as described below.

## 3. Procedure

The procedure described herein can be used to quantify axial deformation of vertical structural components in structural framing system.

1. Prior to the application of axial loads, the modal parameters of natural frequencies and mode shapes of a structure can be obtained from the outputs of accelerometers, as well as from modal analysis of an FE model (FEM) of the structure.

2. Comparing the two sets of results, the FEM can be validated and $F_{xu}$ for element *x* can be calculated using Eq. (28) and retained for future use. By applying known axial loads to both the FEM and the real structure, the above procedure can be repeated to improve the model validation.

3. In the next stage, the validated FEM of the structure is used to develop a database that relates the index *SI* to the axial deformation (*AD*). For a given axial load applied to the FEM of the structure, the modal parameters are determined using the modified FE program and the $F_{XL}$ is first calculated using Eq. (29) and then along with the $F_{XU}$ determined earlier, *SI* for the particular case is calculated using Eq. (32). Axial deformation due to this axial force can also be obtained from static analysis. Repeating this procedure for a range of axial loads, a database for SI vs AD can be generated.

4. Using the results from the database developed in the step above, graphs with the vertical axis representing the Stiffness Index (*SI*) and the horizontal axis representing the axial deformation

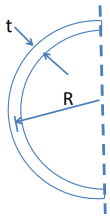


Fig. 2 Cross section of the beam

Table 1 material properties and other data used in the vibration analysis

| Beam Parameter | Numerical Value |
|---|---|
| R(mm) | 24.5 |
| t(mm) | 4 |
| L(mm) | 820 |
| m(Kg/m) | 0.835 |
| E(GPa) | 68.9 |
| G(GPa) | 26.5 |

(*AD*), can be plotted for each element *x* in the structural framing system. As will be seen later, the variation of *SI* with *AD* will be linear. It is hence evident that, if *SI* is known (at any stage of loading or construction of the structure) the axial deformation (*AD*) can be obtained by applying either interpolation or extrapolation methods.

5. During the service life of a structure, the axial deformation (*AD*) of any element can be obtained from the *SI* vs *AD* graphs, if the current *SI* is known. Under an unknown axial load on the real structure, the modal parameters amend and they can be extracted from the deployed accelerometers and then used to calculate the current *SI* as described earlier. The axial deformation (*AD*) corresponding to the unknown axial load can then be obtained from the already available graphs of *SI* vs. *AD* for that element.

## 4. Validation and Illustrative example.

Three numerical examples are presented in this section. The first example is for validating the FE program with the preprocessing technique developed in this research to incorporate the effect of axial load into vibration characteristics while the other examples are used to illustrate the proposed procedure described in Section 3 and its capabilities.

### *4.1 Example 1*

Banerjee and Williams (1994) carried out comprehensive studies on an axially loaded beam with cantilever end condition using different approaches. This example is used to evaluate the accuracy of the technique developed in this paper. Fig. 2 shows a cross section of a beam while Table 1 presents the material properties and other data used in the vibration analysis. More information on the selected element can be found in (Banerjee and Williams 1994).

Table 2 comparison of natural frequencies without axial load

| Natural Frequency (rad/s) | | | |
|---|---|---|---|
| Axial force=0 | | | |
| Frequency Number | Banerjee and Williams | This Research | Variations (%) |
| 1 | 391.70 | 390.40 | 0.33 |
| 2 | 816.00 | 815.00 | 0.12 |
| 3 | 1629.00 | 1625.00 | 0.25 |

Table 3 comparison of natural frequencies with tension axial load

| Natural Frequency (rad/s) | | | |
|---|---|---|---|
| Axial force=−1790 N (tension) | | | |
| Frequency Number | Pervious Publications [9] | This research | Variations (%) |
| 1 | 405.80 | 404.00 | 0.44 |
| 2 | 826.70 | 826.00 | 0.08 |
| 3 | 1649.00 | 1650.00 | 0.06 |

Table 4 comparison of natural frequencies with compression axial load

| Natural Frequency(rad/s) | | | |
|---|---|---|---|
| Axial force=1790N(compression) | | | |
| Frequency Number | Pervious Publications [9] | This research | Variations (%) |
| 1 | 376.80 | 377.00 | -0.05 |
| 2 | 805.10 | 804.00 | 0.14 |
| 3 | 1609.00 | 1608.00 | 0.06 |

A finite element model of this structural component was developed using the FE program and was first subjected to an axial compressive force of 1790N and then to an axial tensile force of the same magnitude. These are the loads used in the previous publication (Banerjee and Williams 1994). The natural frequencies of the first three modes and the corresponding mode shapes with and without axial loads are extracted from the analysis results and compared with results from the previous publication. Tables 2 to 4 show the results for the natural frequencies of the first three modes for the three cases.

It is evident that the present results compare well with those from Banerjee and Williams (1994). In additions, the 1$^{st}$ three mode shapes obtained from the present analysis, where the first mode is bending and the next two modes are mostly torsional, also compare well those from the previous research and highlight the accuracy of the finite element modeling and the preprocessing techniques developed and used in this research.

### *4.2 Example 2*

A column, 0.5×0.5×4 m with different boundary conditions is selected to illustrate capabilities of the proposed procedure. The column was modeled using solid elements to capture torsion, if any, due to the boundary conditions. The material properties of the column are presented in Table 5. 10 axial compressive load cases with loads ranging from 1, 2, 3 up to 10 MN are applied to the column to cause axial deformations in the linear elastic region. Effects of the boundary conditions

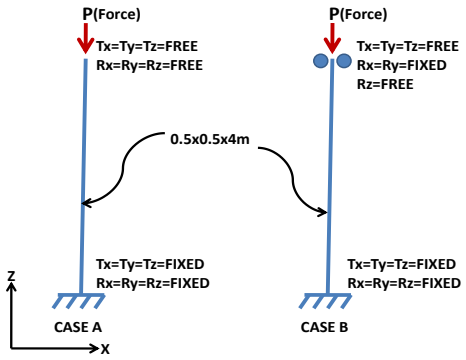


Fig. 3 Columns with two different boundary conditions

Table 5 material properties of the column

| Material Property | Numerical Value |
|---|---|
| Density/(kNm-3) | 2300 |
| Poisson Ratio | 0.2 |
| Young's Modulus /(GPa) | 30 |

are studied using two cases; A and B shown in Fig. 3. The first three frequencies and the associated modes were obtained for both cases from the modal analyses of the FE models.

#### *4.2.1 Case A: results and discussion*

The results indicated that first and second modes are bending while the third mode is a combination of bending and torsional. The frequency changes for each mode due to the axial compressive force are depicted in Fig. 4. It is interesting to note that this change is largest for the first mode and reduces with the mode number and shows that the stiffness matrix change under axial force can be captured by using the first mode. Similar observations were made in a previous study (Della and Shu 1975).

For each axial force the modal parameters (natural frequencies and modal vectors) were obtained from the finite element analysis and Eqn (32) was used to calculate the Stiffness Index; *SI*. The corresponding axial deformation was obtained using static analysis. Fig. 5 shows the variations of *SI* with the axial deformation for three different cases – using the (i) first mode, (ii) first two modes and (iii) first three modes.

It is clearly revealed from Fig. 5 that *SI* does not deviate significantly with an increase in the number of modes incorporated into the calculation. This confirms that impact of number of modes on case A is very low. Fig. 5 also shows that the variations are linear and enable interpolation and extrapolation methods to estimate the axial deformation due to an unknown applied axial force, if the *SI* can be obtained from vibration measurements – the essence of the proposed methodology.

#### *4.2.2 Case B: results and discussion*

For case B, the frequency changes with axial loads are similar to those in case A with the

largest change for the first mode. However, the mode shapes for case B seem to be different to case A due to the impact of the different boundary conditions (see Fig. 3). Though the first two modes are bending while the third mode is a combination of bending and torsional, as also observed for case A, the shapes of the modes for case B are different from those for case A. It was also observed that there was a significant change in the first mode shape due to the influence of the axial load as also observed by Della and Shu (1975).

Fig. 6 shows variation of stiffness index, *SI* with the axial deformation, *AD* where the impact of number of modes can be examined. In case B, the boundary conditions influence the variation of

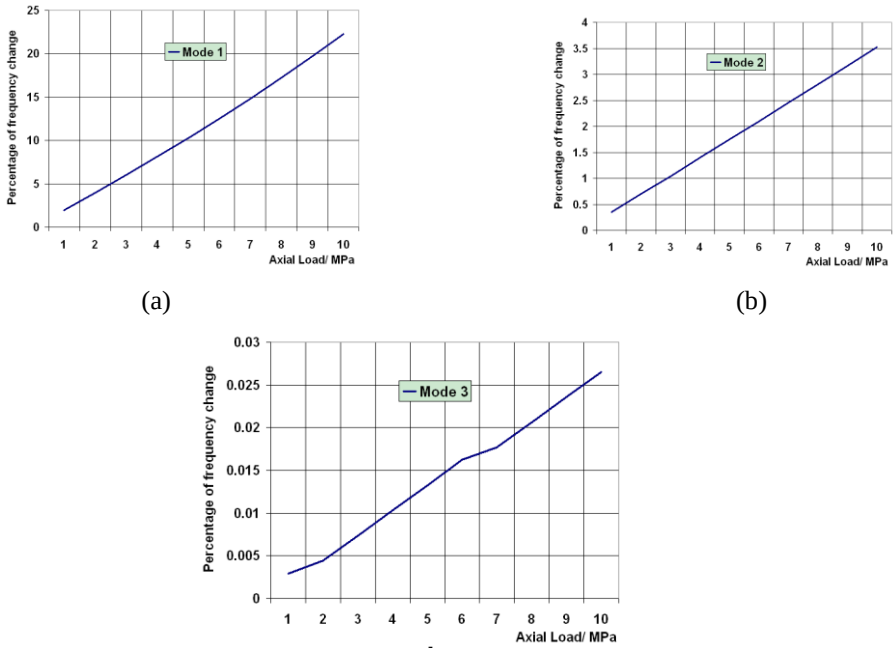


Fig. 4 Percentage of frequency change (a) first mode, (b) second mode and (c) third mode

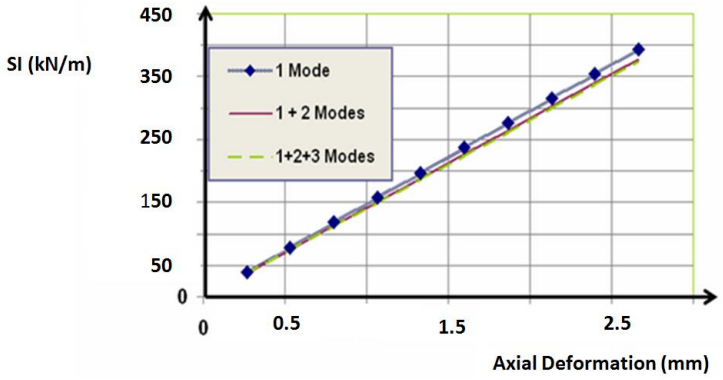


Fig. 5 variation of stiffness index, SI with the axial deformation for case A

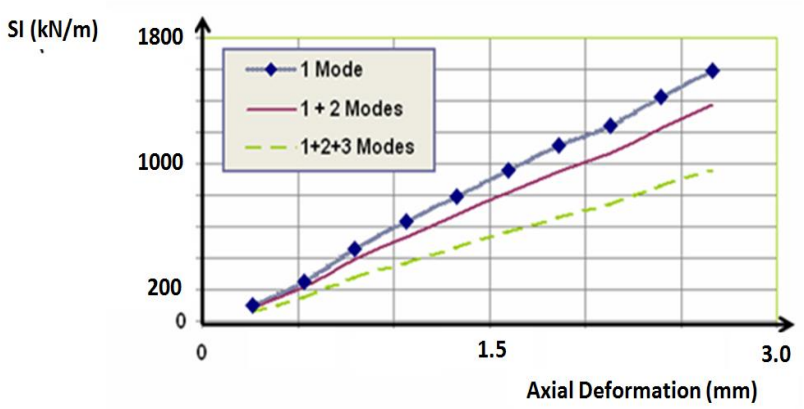


Fig. 6 Variation of stiffness index, SI with the axial deformation for case B

the mode shapes and hence *SI*. Consequently, the graphs (see Fig. 6) deviate considerably when the number of modes used in the calculation is increased. This feature is different to that observed for case A and highlights the effect of boundary conditions on the *SI* proposed in this paper.

### 4.3 Example 3

As the last example, a 10 storey structural framing system with shear walls is used to illustrate the capability of the Stiffness Index (*SI*) and the proposed procedure to capture load migrations among members. The material properties of all structural components are selected to be same as in the previous example. Sizes of columns and beams are 1×1 m and 0.3×0.5 m respectively while 0.5m thickness shear walls are located as shown in Fig. 7. Because of the shear walls, load migration occurs among the columns as in a structural framing system with belt and outrigger systems which are commonly used in structural framing systems of high rise buildings. This example studies the capability of the proposed *SI* to capture effects of load migration. Floor height of the selected structure is 4m. Different axial compressive loads are applied on columns as shown in Table 6. These loads facilitate to simulate different loads on the vertical structural components due to different load tributary areas, and are increased by 0.25MN to develop several loading cases. Stiffness Indexes, *SI*(s) of columns C1, C2, C3 and C4 in Fig. 7 at certain floor levels are selected to examine their behavior. *SI*(s) of columns in floor levels 2 6 and 10 represent their behavior at lower, middle and upper levels respectively, while *SI*(s) of columns in levels 4 and 8 represent the behavior under load migration occurring due to shear walls located in these levels.

Separate modal analyses are performed incorparating the effects of the applied axial compressive loads for each loading case using the developed and validated preprocessing technique. The first two modes of vibration, both of which are bending modes, and the corresponding frequencies are extracted from the analyses to calculate *SI*(s) of columns, as higher modes do not impact significantly on *SI* as indicated in the previous examples. Stiffness Indexes, *SI*(s)) are calculated for each column at the selected floor levels using the results from the modal analyses, while static analyes are used to calculate the axial deformations of the columns. Fig. 8 shows the variation of the *SI*(s) of the columns with their axial deformations at the selected floor levels.

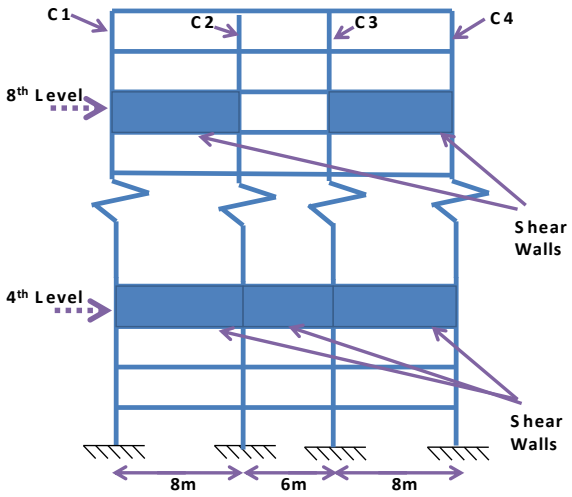


Fig. 7 Structural framing system with shear walls

Table 6 Initially applied axial compressive loads on columns

| Floor Number | Force/ MN | | | |
|---|---|---|---|---|
| | Column | | | |
| | C1 | C2 | C3 | C4 |
| 1 | 1 | 1.5 | 2 | 1 |
| 2 | 1 | 1.5 | 2 | 1 |
| 3 | 2 | 3 | 3.5 | 2 |
| 4 | 1 | 1.5 | 2 | 1 |
| 5 | 1 | 1.5 | 2 | 1 |
| 6 | 1 | 1.5 | 2 | 1 |
| 7 | 2 | 2.5 | 3 | 2 |
| 8 | 1 | 1.5 | 2 | 1 |
| 9 | 1 | 1.5 | 2 | 1 |
| 10 | 1 | 1.5 | 2 | 1 |

Figs. 8 (a), (c) and (e) depict that *SI* of column C3 is lower than that of the other columns while *SI* of column C2 is lower compared to columns C1 and C4. This is because column C3 is subjected to a higher axial compressive load than others and column C2 is subjected to a higher axial load than that of columns C1 and C4 (see Table 6).

Load migration can occur from a column with a larger axial load to column(s) with smaller axial load(s) when these columns are connected by stiff shear walls. The capability of *SI* to capture these load migrations among columns can be seen in Figs. 8(b) and 8(d). *SI* of column C1 is higher compared to that of column C4 at levels 4 and 8 though these two columns are subjected to equal axial loads (see Table 6). At the 4$^{th}$ level, axial load of column C3 migrates to columns C4 and C2 via the shear walls while the axial load of column C2 migrates only to column C1 via the shear wall. Load migration from column C3 to C4 is higher than that from column C2 to C1 since the

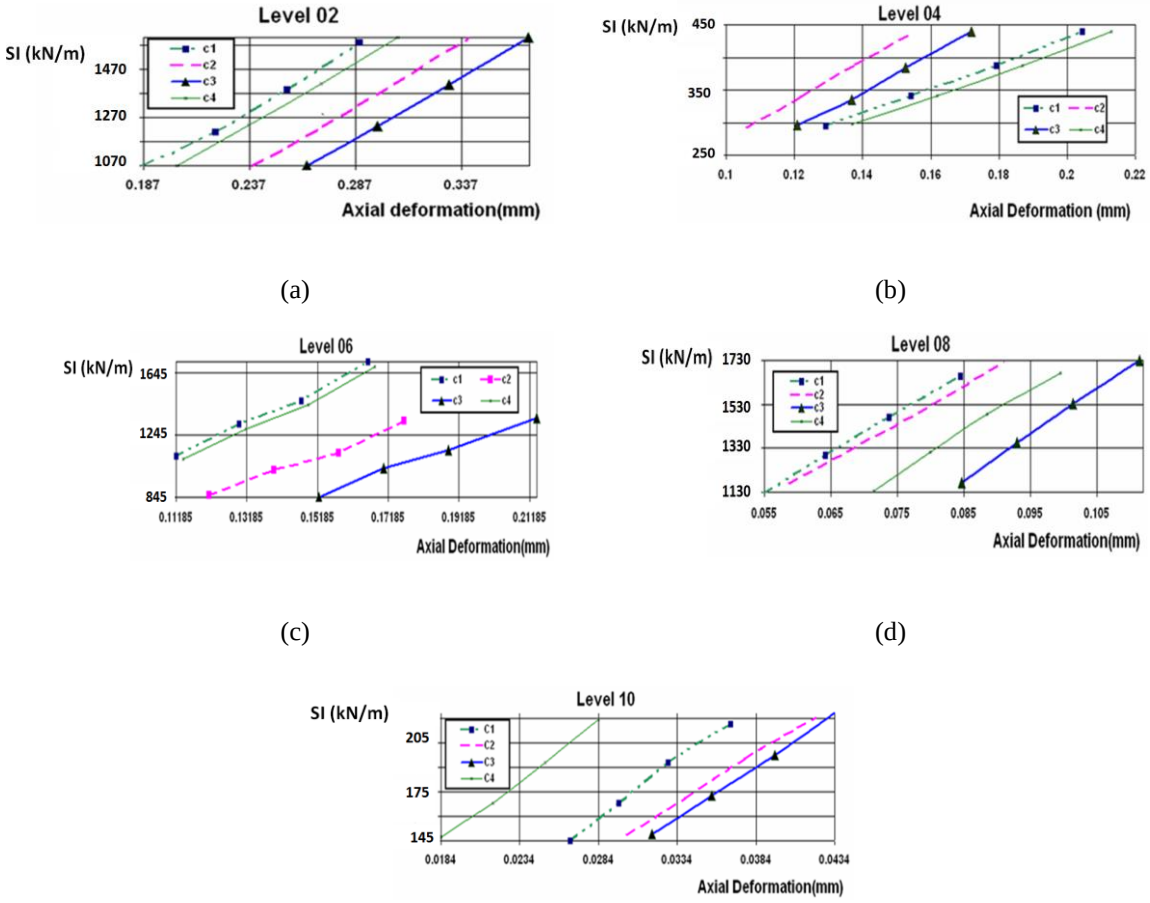


Fig. 8 variation of SI(s) of the columns, (a) 2nd level, (b) 4th level, (c) 6th level, (d) 8th level and (e) 10th level

axial load of column C3 is higher than that of column C2. Hence C4 acquires more load than column C1 and Fig. 8(b) depicts that *SI* of column C4 is lower than that of column C1. It is also seen that SI of column C1 is lower than that of columns C2 and C3 from which load migrations occur to the outer columns. The shear wall configuration at the 8$^{th}$ level is different to that at the 4$^{th}$ level (see Fig. 7). Axial load of column C3 migrates to column C4 while axial load of column C2 migrates to column C1. However, axial load of column C3 is higher than that in the other columns so that load migration from columns C3 to C4 is higher than that between the other two columns. Axial deformation of column C4 is thereby more pronounced than that of columns C1 and C2 and hence *SI* of column C4 is lower in comparison to that of columns C1 and C2 as shown in Fig. 8(d).

Moragaspitiya *et al.* (2010) reported that even though the axial (elastic) deformations are low, they impact significantly on the creep deformations which are long term time dependent phenomenon. Accurate quantification of the axial deformations, incorporating load migration

among the vertical load bearing structural components, are hence essential in order to provide adequate provision to mitigate the adverse effects of differential axial deformations such as tilting of horizontal floor plates, deformation of claddings and facades, etc.

Figs. 5, 6, and 8 indicate linear variations of *SI* with axial deformation for the different structural components confirming that interpolation and extrapolation methods can be used to calculate the axial deformation due to unknown axial loads, when the *SI* is determined from vibration measurements. These linear graphs show that as the axial deformations of the components are in the linear elastic range, their stiffness reduces linearly. When axial deformation due to an unknown axial force is needed, modal vectors and natural frequencies can be obtained from the deployed accelerometers and the stiffness index, *SI* can be calculated. The axial deformation can then be obtained by using interpolation and extrapolation methods on the graph, as explained in step 5 of the procedure described in section3.

## 6. Conclusions

Numerous methods have been developed to relate axial force and hence axial deformation of a single structural component using its natural frequencies. These developments cannot be applied to a structural component in a structural framing system since the natural frequency is a property of the entire structural framing system, and they are not capable of capturing the load migration among vertical structural components due to the presence of horizontal stiff structural systems such as belt and outrigger systems. In response to the need for a rigorous method to quantify axial deformation of vertical load bearing structural components of structural framing systems, a comprehensive method incorporating a vibration based parameter called stiffness index (*SI*) is proposed in this paper and illustrated through examples. Results indicate that the proposed procedure has the ability to quantify axial deformations of structural components in a structural framing system and capture the effects of the magnitudes of axial loads, the boundary conditions and the load tributary areas as well as the load migration. The method proposed in this paper can be used to quantify axial deformation of vertical structural components of a complex structural framing system under gradual loadings using a non destructive vibration based test.

## References

Adewuyi, A.P. and Wu, Z.S. (2010), "Modal macro-strain flexibility methods for damage localization in flexural structures using long-gage FBG sensors", *J. Struct. Control Hlth. Monit.*, **18**(3), 341-360.

ANSYS 13-SP2-© -SASIP Inc. (2011), Manual, Ansys Inc., Canonsburg, PA.

Banerjee, J.R. and Williams, F.W. (1994), "Coupled bending-torsional dynamic stiffness matrix of an axially loaded Timoshenko beam element", *Int. J. Solid Struct.*, **31**(6), 749-762.

Bahra, A.S. and Greening, P.D. (2008), "Identifying axial load patterns using space frame FEMs and measured vibration data", *J. Mech. Syst. Signal Proc.*, **23**, 1282-1297.

Catbas, F.N., Brown, D.L. and Aktan, E. (2006), "Use of modal flexibility for damage detection and condition assessment: case studies and demonstrations on large structures", *J. Struct. Eng., ASCE*, **132**, 699-1711.

Della, C.N. and Shu, D. (1975), "Free vibration analysis of multiple delaminated beams under axial compressive loads", *J. Reinf. Plastic. Compos.*, **28**, 1365-1380.

Friberg, P.O. (1985), "Beam element matrices derived from vlasov's theory of open thin walled elastic

beams", *Int. J. Numer. Method. Eng.*, **21**, 1205-1228.
Jahanshahiya, M.R. and Rahgozar, R. (2012), "Free vibration analysis of combined system with variable cross section in tall buildings", *Struct. Eng. Mech.*, **42**(5), 715-728.
Kisa, M. (2012), "Vibration and stability of axially loaded cracked beams", *Struct. Eng. Mech.*, **44**(3), 305-323.
Moragaspitiya, H.N., Thambiratnam, D.P., Perera, N.J. and Chan, T.H.T. (2010), "A numerical method to quantify differential axial shortening in concrete buildings", *J. Eng. Struct.*, **32**(8), 2310-2317.
Shaker, F.J. (1975), "Effect of axial load on mode shape and frequencies of beams", *NASA (National Aeronautics and Space Administration)* Technical Mote, NASA TN-D-8109.
Shih, H.W., Thambiratnam, D.P. and Chan, T.H.T. (2009), "Vibration based structural damage detection in flexural members using multi-criteria approach", *J. Sound Vib.*, **323**, 645-661.
Walter, D. and Kang, W. (1996), "Exact stiffness matrix for a beam element with axial force and shear deformation", *J. Finite Elem. Anal. Des.*, **22**, 1-13.
West, H.H. and Geschwindner, L.F. (2002), *Fundamentals of Structural Analysis*, 2nd edition, John Wiley & Sons Ltd. (2002)
Yesilce, Y. and Demirdag, O. (2008), "Effect of axial force on free vibration of Timoshenko multi-span beam carrying multiple spring mass systems", *Int. J. Mech. Sci.*, **50**, 995-1003.
Zhao, J. and Dewolf, J.T. (2006), "Sensitivity study for vibration parameters used in damage detection", *J. Struct. Eng.*, **25**, 410-416.